Novel Aspects in the Structure of Poly(ethylene terephthalate) As Revealed by Means of Small-Angle X-ray Scattering

C. Santa Cruz, N. Stribeck, and H. G. Zachmann

Institut für Technische und Makromolekulare Chemie, University of Hamburg, Bundesstrasse 45, 2000 Hamburg 13, FRG

F. J. Baltá Calleja*

Instituto de Estructura de la Materia, C.S.I.C., Serrano 119, Madrid 28006, Spain

Received January 31, 1991; Revised Manuscript Received June 17, 1991

ABSTRACT: The absolute intensity of the small-angle X-ray scattering (SAXS) of poly(ethylene terephthalate) (PET) samples crystallized at different temperatures for different times was measured by means of a Kratky camera. The correlation function and the interface distribution function were calculated, and the values obtained from different methods for the long period L, the crystal thickness, l_c, the thickness of the amorphous regions l_a, and the linear degree of crystallinity x_{CL} were compared with each other. After a critical examination of the different methods, including model calculations of the interface distribution function and the correlation function, it is shown that, in the case of a broad distribution of thicknesses, the interface distribution function gives the more reliable results for l_c, l_a, and L. By comparing the linear degree of crystallinity x_{CL} determined from SAXS with the degree of crystallinity x_c as determined from wide-angle X-ray scattering or from density, it is concluded that the material is not homogeneously filled with lamellar stacks. The coherently scattering lamellar stack consists of only 3–6 lamellae.

Introduction

Small-angle X-ray scattering (SAXS) is a powerful tool for the determination of structural parameters of semicrystalline polymers. From the angular position of the maximum of the scattering, the long period, L, can be determined by application of Bragg's law. L is the sum of the average thickness of the crystal lamellae, l_c, and the amorphous regions between these lamellae, l_a. In a more elaborate evaluation the linear correlation function of an isotropic polymer

$$\gamma_1(x) = \frac{2\pi}{Q}\int_0^\infty s\frac{J(s)}{V}[J_0(2\pi xs) - 2\pi xsJ_1(2\pi xs)]\,ds \quad (1)$$

can be calculated,[1,2] where $J(s)$ is the smeared SAXS intensity as measured by a Kratky camera, V is the scattering volume of the sample, $s = 2\sin(\theta)/\lambda$ is the value of the scattering vector, and J_0 and J_1 are Bessel functions. Q is the so-called invariant, which is determined by integrating the SAXS over all scattering angles

$$Q = 2\pi\int_0^\infty s\frac{J(s)}{V}\,ds \quad (2)$$

As a consequence of normalization by Q, the correlation function becomes 1 at $x = 0$; i.e., $\gamma_1(0) = 1$. From the correlation function, in addition to L the values of l_c, l_a, the degree of crystallinity within the lamellar stacks, x_{CL}, and the thickness of the phase boundary between a crystal and the adjacent amorphous region, t, can be calculated by the methods given by Vonk and Kortleve[1,2] and by Strobl and Schneider.[3] Q is, in addition, related to the structure of an ideal two-phase model by means of the equation

$$Q = x(1-x)\Delta\rho^2 \quad (3)$$

x being the volume fraction of one phase and $\Delta\rho$ the electron density difference between the two phases.

Instead of $\gamma_1(x)$ one can also calculate the interface distribution function introduced by Ruland.[4]

$$g_1(x) = \frac{\pi}{4}\int_0^\infty G(s)[3J_0(2\pi xs) - J_2(2\pi xs) + \pi xs(J_3(2\pi xs) - 3J_1(2\pi xs))]\,ds \quad (4)$$

where $G(s)$ is the interference function of the two-phase system.

This function, actually, is the second derivative of the correlation function, $g_1(x) = \gamma_1''(x)$ and represents the probability distribution of finding two interfaces (between a crystal and the adjacent amorphous region) at a distance x. The values of $g_1(x)$ are negative if the sequence of the phases is the same at both considered interfaces, as for example in the case of the distance representing the long period, and are positive if the sequence is not the same, as for example for the distance denoting the crystal thickness. As shown by Stribeck and Ruland[5] by an analysis of this function one can obtain L, l_c, l_a, x_{CL}, t, and the breadth of the distribution of L, l_c, and l_a.

Poly(ethylene terephthalate) (PET) is a suitable material to carry out structural investigations by means of SAXS. By varying the temperature and time of crystallization, states of different crystalline perfection are obtained which can be frozen-in by quenching the sample from the crystallization temperature to room temperature.[6–9] Different authors have investigated the dependence of the long period and of the invariant on the time and temperature of crystallization.[10–14] Measurements of the absolute SAXS intensity have been performed by Konrad and Zachmann[15] and by Fisher and Fakirov.[16] From these measurements the invariant (scattering power) Q was determined and conclusions were drawn concerning the degree of crystallinity and the density difference between the crystalline and amorphous regions. However, as far as we know, up till now no calculation of the correlation function $\gamma_1(x)$ has been performed for PET.

0024-9297/91/2224-5980$02.50/0

The object of the work presented here is to report the study of the correlation function on PET samples crystallized under different conditions and to compare these results with those obtained from the evaluation of the interface distribution function. A critical discussion of the results obtained by the different methods is given. For a more detailed interpretation of the results the invariant was also calculated. Conclusions on the lamellar structure are drawn. It is shown that such a study on PET is of special interest because (1) the variation of crystal thickness within the lamellar stacks is comparatively broad for this polymer and, as a consequence, the evaluation of the SAXS results by simply applying Bragg's law gives inaccurate results and (2) even at the end of the isothermal crystallization, the material is not completely filled up by lamellar stacks.

Experimental Section

PET was synthesized from dimethyl terephthalate and ethylene glycol with manganese acetate and Sb_2O_3 as catalysts as described in an earlier publication.[9] The molecular weight was determined by viscometry with hexafluoro-2-propanol as a solvent and using[17] the equation

$$[\eta] = 5.2 \times 10^{-4} M_w^{0.695} \tag{5}$$

M_w was found to be 33 000. Amorphous films were obtained by melt pressing in vacuo for 10 min at 280 °C and quenching in ice water. The amorphous samples were crystallized in vacuo at three different temperatures (120, 190, and 240 °C) for three different times at each temperature, namely, 1, 9, and 24 h. From previous investigations[6,7] it is known that spherulitic growth is completed in these samples.

The density, ρ, of the samples was measured in a density gradient column containing a mixture of hexane and tetrachloroethane. The volume degree of crystallinity, x_c, was calculated by using the equation

$$x_c = \frac{\rho - \rho_a}{\rho_c - \rho_a} \tag{6}$$

The density of the amorphous regions, ρ_a, was assumed to be 1.338 g/cm^3 and that of the crystals, ρ_c, to be 1.490 g/cm^3. As was shown earlier,[9] the values for the crystallinity determined in this way agree well with values obtained from wide-angle X-ray scattering after applying the method of Ruland.

The SAXS intensity was measured in a Kratky compact camera using Ni-filtered Cu Kα radiation and a proportional counter with energy discrimination as a detector. To determine the scattering intensity appropriately two different widths of the entrance slit were chosen, namely, 60 and 130 μm for $0.013 < s < 0.4$ nm^{-1} and $0.3 < s < 1$ nm^{-1}, respectively. The adsorption factor and the primary beam power per unit slit length were measured by using the moving-slit method.[18]

Method of Evaluation

Determination of the Interface Distribution Function. In the determination of the interface distribution function $g_1(x)$ we consider that crystalline PET is not an ideal two-phase system just consisting of crystalline and amorphous regions but that there also exists a phase boundary of finite thickness t. In addition, we take into account that local electron density fluctuations are present in both regions. The measured scattering curve was corrected with respect to the deviations caused by the two above-mentioned contributions. Thus, the scattering of the corresponding ideal two-phase system, a system which has sharp phase boundaries and a uniform density within each phase, can be obtained. In what follows, in addition to $g_1(x)$, we also have determined the thickness, t, of the phase boundary and the amount of the local density fluctuations J_{Fl}.

The method used is based on investigations by Ruland[4] and Koberstein, Morra, and Stein.[19] The variational process by which J_{Fl} and t are determined is carried out in the following way:

1. The data are plotted in a ln $[s^3(J(s) - J_{Fl})]$ vs $s^{1.81}$ diagram[19] (Figure 1), which is based on an empirical approximation for the smeared scattering of an infinite-length slit using a model with Gaussian phase boundaries

$$J(s) - J_{Fl} \approx \frac{A_P}{s^3} e^{-38(\sigma s)^{1.81}} \tag{7}$$

where σ is the variance of the Gaussian phase boundary and A_P is Porod's asymptote. The width of the phase boundary t is, then, defined as 3σ.

2. The value of J_{Fl} is varied until the range in which the data follow a linear decrease is maximized.

3. A straight line is fitted to the data in this range. The value of Porod's asymptote A_P and σ are obtained from the intercept and slope of the straight line, respectively.

4. With the parameters A_P, σ, and J_{Fl} obtained in this way, the interference function $G_{id}(s)$ of the ideal two-phase system is calculated from the measured scattering intensity $J(s)$ by using Ruland's formula

$$G_{id} = \frac{(J(s) - J_{Fl})s^3}{(1 - 8\pi^2\sigma^2 s^2)\,\mathrm{erfc}\,(2\pi\sigma s) + 4(\pi\sigma s)^{1/2}\exp(-4\pi^2\sigma^2 s^2)} - A_P \tag{8}$$

In contrast to eq 7, this formula holds strictly and does not involve any approximation. If at large values of s, the curve representing $G_{id}(s)$ is not parallel to the s axis, the parameter σ is corrected by performing finer variations of J_{Fl}, A_P, and σ. Furthermore, the parameter A_P is adjusted so that $G_{id}(s)$ approaches zero for large values of s. From this equation one can obtain the interface distribution function by means of eq 4.

5. The scattering of the ideal two-phase system with sharp transitions between the two phases and a uniform electron density within each phase $J_{id}(s)$ can be calculated from the $G_{id}(s)$ by means of the equation

$$G_{id}(s) = 16\pi^2\left[s^3\frac{J_{id}(s)}{V} - A_P\right] \tag{9}$$

The interface distribution function $g_1(x)$ is obtained by inserting $G_{id}(s)$ from eq 9 into eq 4.

Evaluation of the Interface Distribution Function. If l_c, l_a, and $L = l_c + l_a$ were constant throughout the whole sample, the interface distribution function would, then, consist of several δ functions with positive and negative signs. The appearance of a smooth curve indicates that there exist more or less broad distributions of these values. For further evaluation we assume Gaussian distributions for l_c, l_a, L, $L + l_c$, and so on and determine the values of l_c, l_a, and L as well as the variances of these values by fitting the experimental curves as shown in Figure 2. The attempt to assume distribution functions only for l_c and l_a and to calculate the other distribution functions by convolution integrals does not lead to a good fit between the experimental and the theoretical curves. Therefore, the values obtained for the variances seem to use the subject for a more detailed investigation. The results will be reported in a separate publication.[21] Hence in the present paper, we will confine our attention to the average values for l_a, l_c, and L and to the comparison of these values to those obtained from the correlation function.

From the interface distribution function it is not possible to distinguish which one of the two characteristic lengths

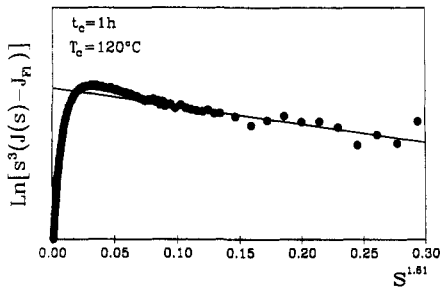

Figure 1. Stein plot to obtain the electron density fluctuation, J_{Fl}, the width of the phase boundary, t, and Porod's asymptote, A_P (ref 19) for the sample crystallized at T_c = 120 °C and t_c = 1 h.

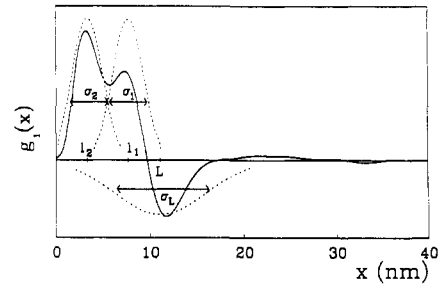

Figure 2. Interface distribution function derived from the correlation function of Figure 3 illustrating the different length distributions.

is l_c and which one is l_a. Therefore, we denote the larger length l_1 and the smaller one l_2. Consequently, the fraction of the phase which is present in the lamellar stacks in a larger amount is given by

$$x_1 = \frac{l_1}{l_1 + l_2} = \frac{l_1}{L} \tag{10}$$

Determination of the Correlation Function. Before performing the Fourier transform in eq 1, we subtracted the contribution of the local electron density fluctuations J_{Fl} from the measured scattering intensity and extrapolated the latter to $s = \infty$ by applying Porod's law. Following the procedure used by other investigators who calculated the correlation function,[1-3] no correction with respect to the finite phase boundary thickness was performed. As a consequence, $J_{id}(s)$ given by eq 9 could not be used. Instead, we have just subtracted J_{Fl} as determined by the procedure described by Koberstein, Morra, and Stein.[19] In contrast to the above procedure,[1-3] we have used for the invariant Q (eq 2) the value obtained for the corresponding ideal two-phase system with a finite phase boundary. As was shown by other authors,[1-3] if $\gamma_1(x)$ is normalized in this way, one obtains $\gamma_1(0) < 1$. The straight line fitted to $\gamma_1(x)$ in the region $x \geq 0$ has the intercept 1 at the ordinate. This is of help in fitting this line which is required for further evaluation and justifies the normalization used. When we normalize the correlation function by using the invariant Q, it is important to perform the extrapolation of $J(s)/V$ to large s values because they may contribute up to 20% to the Q value, as was shown by Ruland.[4] The corrections seems to be not so important for the determination of the shape of the correlation curve. It is worth pointing out that Vonk[2] did not use the same normalization as we do in the present study. According to his normalization $\gamma_1(0) = 1$.

Determination of the Structural Parameters from the Correlation Function. There are different possibilities to determine the structural parameters from the correlation function. On the one hand, the long period, L, can be determined from the position of the first maximum in the correlation function (see Figure 3). This value represents the most probable distance between the centers of gravity between two adjacent crystals. We will denote the L values determined in this way by L_C^M. On the other hand, L can be determined as twice the value obtained from the first minimum of the correlation function which is interpreted as the most probable distance between the center of gravity of a crystal and its adjacent amorphous region. The value determined in this way will be denoted L_C^m. If the lamellae form a one-dimensional ideal lattice, both values coincide. However, if this superlattice is not ideal, the position of the maximum, L_C^M, and of the minimum, $L_C^m/2$, in the correlation function may be slightly shifted. As a consequence, different L values may be obtained by the two methods.

Another important parameter is the degree of crystallinity within the lamellar stacks, the so-called linear crystallinity, x_{CL}. This quantity cannot be determined from the correlation function alone because it cannot be distinguished from the amorphous fraction $1 - x_{CL}$. Therefore, we denote the larger fraction of the two phases by x_1 and the smaller one by x_2. There are two methods[2] to determine x_1:

1. From the equation

$$\frac{1 - x_1}{x_1} = cy \tag{11}$$

where y is the value of the correlation function at its first minimum (see Figure 3) and c is a factor determined in such a way that $c\gamma_1(0) = 1$. The factor c is introduced as a consequence of our normalization of the correlation function. In the paper of Kortleve and Vonk[1] where $\gamma_1(x)$ is normalized in such a way that $\gamma_1(0) = 1$, the constant $c = 1$.

2. From the equation

$$x_1(1 - x_1)L_C^M = A \tag{12}$$

where A is the first intercept of the correlation function with the abscissa. The values determined in this way will be denoted by $x_1°$.

Finally, the thickness of the crystals, l_c, and that of the amorphous regions, l_a, may be determined. Again, as in the case of the interface distribution function, it is not possible to distinguish between l_c and l_a. We, therefore, designate the larger thickness by l_1 and the smaller one by l_2. We can then obtain these quantities from the values of L and x_1 by means of the equations

$$l_1 = x_1 L \tag{13}$$

and

$$l_2 = (1 - x_1)L \tag{14}$$

Furthermore, l_2 can also be derived[2] by means of the equation

$$l_2 \approx B \tag{15}$$

where B is defined in Figure 3.

If l_2 is determined by eq 15, there arises a new possibility to obtain $1 - x_1$ by using eq 14. This method was used by Strobl et al.[3] The value determined in this way will be called x_{1L}.

Results

Figure 4 shows the scattering curves of a PET sample crystallized at 240 °C for different times (top) and crystallized at different temperatures for 24 h (bottom).

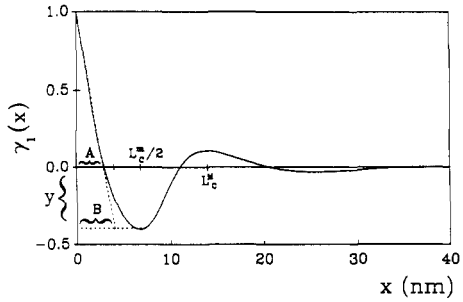

Figure 3. Typical correlation function showing the main parameters to be used (see text).

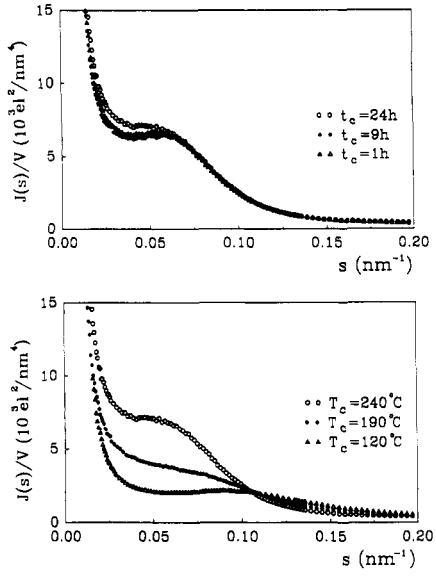

Figure 4. Experimental scattering curves of the PET samples crystallized at 240 °C for different times t_c (top) and crystallized for 24 h at different temperatures T_c (bottom).

Scattering maxima are obtained in all cases. The annealing time does not substantially affect the scattering maximum. However, with increasing temperature the maximum shifts to smaller scattering angles, which corresponds to a change in the long period L_B as determined from Bragg's law.

Figure 5 shows the linear correlation functions obtained from the scattering curves represented in Figure 4. One can observe different positions of the minima and maxima of $\gamma_1(x)$ corresponding to the different positions of the maxima in the scattering curves.

In Figure 6 the interface distribution functions obtained from the scattering curves in Figure 4 are shown. These curves also reveal changes in the position of the minima which correspond to the different long periods appearing in Figure 4.

In Figure 7 the long period, L_B, for a PET sample crystallized at various temperatures for 1 h obtained from the maximum of the scattering curve, after subtraction of the background scattering and application of the Lorentz correction,[20] is compared with the long periods L_C^m and L_C^M obtained from the first minimum and the first maximum of the correlation function, respectively. In addition, the long period obtained from the minimum of the interface distribution function without any correction L_I and the one obtained after doing the separation of the different contributions, L_{IS}, are shown.

As one can see, the values obtained from the interface distribution function are considerably lower. In the case of no overlap correction (curve L_I) the discrepancy is smaller than after performing such a correction (curve L_{IS}). In all cases, a considerable increase of L with

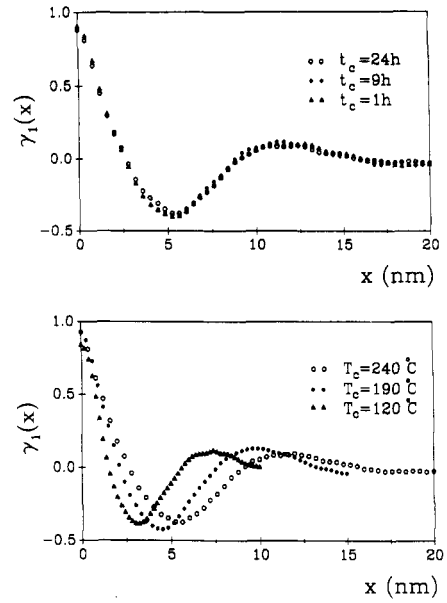

Figure 5. Linear correlation function $\gamma_1(x)$ of the same samples as in Figure 4 crystallized at 240 °C for different times t_c (top) and crystallized for 24 h at different temperatures T_c (bottom).

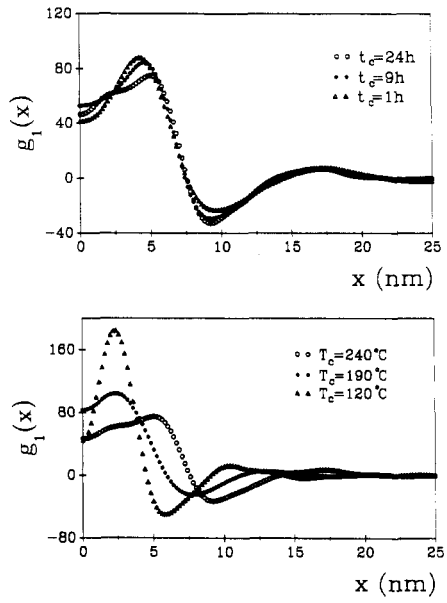

Figure 6. Interface distribution function for the same samples as in Figure 4 crystallized at 240 °C for different times t_c (top) and crystallized for 24 h at different temperatures T_c (bottom).

crystallization temperature T_c is observed. Similar results are obtained in the case of other crystallization times t_c. It is seen that at shorter crystallization times the long periods become slightly smaller. All experimental data are summarized in Table I.

We wish to mention that the values of L_B obtained by applying Bragg's law without brackground subtraction and Lorentz factor corrections are larger by a factor of 1.8 than the L_B values given. This difference may be due to a broad distribution of L values.

Figure 8 shows the fraction x_1 of the phase present in a larger amount within the lamellar stacks as obtained from SAXS using the different evaluation methods (eqs 11, 12, 14, and 10). In addition, the corresponding results for the other crystallization times are presented in Table I.

It is interesting to note that the x_1 values shown in Figure 8 are nearly independent of the temperature of crystal-

Table I
Experimental Values for the Density, ρ, the Volume Degree of Crystallinity, x_c, the Long Period, L, the Larger Thickness, l_1, of the Two Phases, and the Linear Degree of Crystallinity, x_1, Obtained by Using the Different Evaluation Methods[a]

	T_c = 120 °C			T_c = 190 °C			T_c = 240 °C		
t_c, h	1	9	24	1	9	24	1	9	24
ρ, g/cm^3	1.376	1.381	1.382	1.393	1.394	1.396	1.403	1.408	1.416
x_c	0.25	0.28	0.29	0.36	0.37	0.38	0.43	0.46	0.51
L_C^m, nm	6.8	7.2	7.2	9.0	9.0	8.4	12.0	10.4	11.2
L_C^M, nm	7.1	7.0	7.4	10.0	9.4	9.4	12.3	10.8	11.8
L_I, nm	5.6	5.8	5.8	7.8	8.0	7.8	9.8	9.4	9.8
L_{IS}, nm	3.9	5.4	4.9	5.3	7.1	7.3	6.9	7.7	8.2
l_{1C}^m, nm	4.7	5.0	5.0	6.3	5.9	5.4	7.2	7.1	8.0
l_{1C}^M, nm	5.0	5.0	5.4	6.5	6.4	6.4	7.5	7.6	8.0
l_{1IS}, nm	2.7	3.3	3.0	3.5	3.9	4.6	4.7	5.3	5.7
x'_{1m}	0.69	0.69	0.69	0.72	0.67	0.71	0.70	0.68	0.69
$x_1°$	0.70	0.71	0.73	0.75	0.68	0.71	0.74	0.70	0.68
x_{1IS}	0.70	0.61	0.61	0.65	0.66	0.63	0.68	0.69	0.70
x_{1L}	0.69	0.63	0.62	0.64	0.64	0.60	0.65	0.64	0.68

[a] T_c and t_c are the temperature and time of crystallization, respectively.

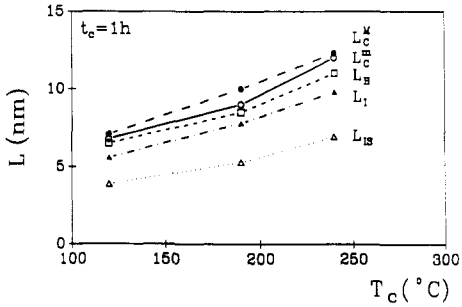

Figure 7. Long periods obtained by different evaluation methods as a function of the crystallization temperatures T_c for the samples crystallized during 1 h. Values obtained from Bragg's law (L_B), from the first maximum (L_C^M) and the first minimum (L_C^m) of the correlation function, and from the interface distribution function without (L_I) and with overlapping corrections (L_{IS}).

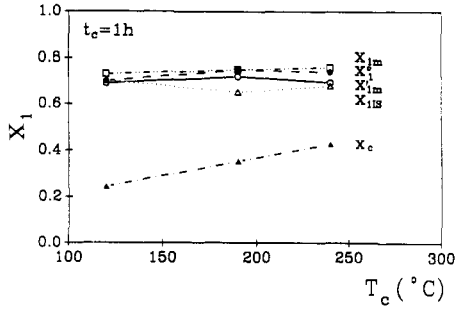

Figure 8. Fraction, x_1, of the phase which is present in the lamellar stacks to a larger amount as a function of crystallization temperature for the sample crystallized for 24 h as determined by means of eq 12 ($x_1°$), by means of eq 11 with $c = 1$ (x_{1m}), by means of eq 11 with $c = 1/\gamma_1(0)$ (x'_{1m}), and from the interface distribution function determined by means of eq 13 (x_{1IS}). The crystallinity measured by density using eq 6 (x_c) is also given.

lization. Neither are they much affected by the method of evaluation. The constancy of x_1 as a function of T_c was already found in an earlier investigation.[15] In contrast, x_c increases with T_c and is always smaller than x_1. If we assume that x_1 represents x_{CL}, this result would suggest that a fraction of the amorphous regions is lying outside of the lamellar stacks in which the crystals are regularly arranged. With increasing crystallization temperature that fraction of these amorphous regions decreases. The other possibility is that x_{CL} is assigned to $1 - x_1$. This alternative holds for the samples crystallized at 120 °C (see Figure 8 and Table I). For the samples crystallized at 190 and 240 °C $1 - x_1$ would be smaller than x_c, an alternative which has no physical meaning.

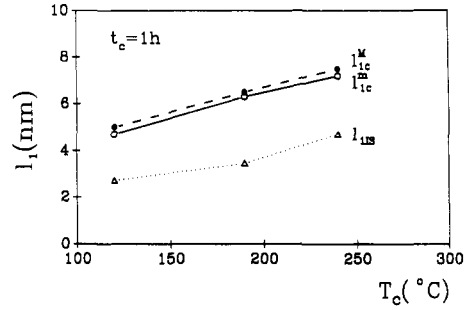

Figure 9. Values of the larger distance, l_1, obtained by using the different methods of evaluation as a function of crystallization temperature for the samples crystallized for 1 h. The values l_{1C}^m and l_{1C}^M are determined from eq 13 and l_{1IS} is determined from eq 10.

Figure 9 represents the thicknesses l_1 as a function of crystallization temperature T_c for a sample crystallized for t_c = 1 h. The values l_{1C}^M and l_{1C}^m designate the crystal thickness obtained from the correlation function by means of eq 13, where L is determined from the first maximum and first minimum of this function, respectively, and x_1 is determined from eq 11. The values of l_{1IS} are determined from the interface distribution function. From this plot and from the data summarized in Table I is is seen that the thickness l_1 increases considerably with increasing crystallization temperatures, T_c, and rises only slightly with crystallization time t_c. The same behavior is observed with l_2.

Finally, we have also determined the invariant Q, the electron density fluctuation J_{Fl}, Porod's asymptote A_P, and the thickness of the phase boundary t (eq 7). The results are presented in Table II. The invariant Q increases with increasing crystallization temperature, while the thickness of the phase boundary, t, and the electron density fluctuation, J_{Fl}, decrease with increasing temperature and crystallization time.

Discussion

Comparison of the Results Obtained by the Different Methods. As clearly demonstrated in Figures 7 and 9, the values of the long period L and of the larger thickness l_1 derived from the interface distribution function are systematically smaller than those calculated from the correlation function. To find out whether this is simply a consequence of a systematic inaccuracy in the mathematical treatment, we have twice integrated the interface distribution function $g_1(x)$; the resulting function is, by

Table II
Experimental Values for the Invariant, Q, Porod's Asymptote, A_P, the Electron Density Fluctuation, J_{Fl}, and the Width of the Phase Boundary, t, for the Different Samples Investigated

	T_c = 120 °C			T_c = 190 °C			T_c = 240 °C		
t_c, h	1	9	24	1	9	24	1	9	24
Q, e²/nm⁶	400	434	410	481	508	473	517	523	567
A_P, e²/nm⁷	5.3	4.1	3.9	3.9	3.5	3.7	3.1	3.3	3.3
J_{Fl}, e²/nm⁴	535	535	510	510	485	482	445	418	436
t, nm	1.05	0.47	0.20	0.25	0.43	0.37	0.39	0.25	0.00

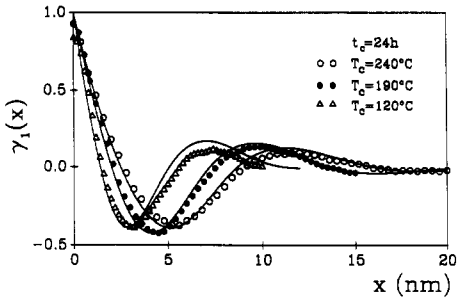

Figure 10. Linear correlation functions obtained by means of eq 1 for the samples crystallized for 24 h at the three different temperatures (data points) and the corresponding correlation functions obtained by double integration of $g_1(x)$ (solid lines).

definition, the linear correlation function. This function will be designated by $\gamma_1^*(x)$ to distinguish it from $\gamma_1(x)$, which we have directly derived from the measured scattering intensity $J(s)$ using eq 1. In Figure 10 the two functions are compared with each other. There is, indeed, a good agreement between the position of the first minimum of $\gamma_1^*(x)$ and $\gamma_1(x)$ as can be also seen in Table IV. Though the minimum of $\gamma_1(x)$ corresponds to a value of L which is a little larger than the one obtained from $\gamma_1^*(x)$, the discrepancy is small in comparison with the difference to the value obtained from the first minimum of the interface distribution function, $g_1(x)$. The difference between the first maximum of $\gamma_1(x)$ and that of $\gamma_1^*(x)$ for each curve is larger than the difference between the position of the minima. However, this discrepancy, too, is small if compared to the difference with respect to L obtained from the interface distribution function.

The small difference between $\gamma_1(x)$ and $\gamma_1^*(x)$, including the behavior of the correlation function at $x = 0$, where $\gamma_1^*(0) = 1$ in contrast to $\gamma_1(0) < 1$, is due to the following reasons: On the one hand, $g_1(x)$ is the interface distribution function of the ideal two-phase system obtained by replacing the phase boundary of finite thickness between crystal and amorphous regions in the real system by sharp boundaries. Since $\gamma_1^*(x)$ is obtained by double integration of $g_1(x)$, it follows that $\gamma_1^*(x)$ represents the correlation function of the corresponding ideal two-phase system with sharp boundaries. In such a system, for $x = 0$ the correlation function is equal to 1 and the first derivative of the correlation function is negative. On the other hand, $\gamma_1(x)$ was calculated from the scattering curve of the real system in which we have subtracted the contribution of the electron density fluctuation J_{Fl}. Therefore, this function represents the real two-phase system with finite phase boundaries normalized by the invariant of the corresponding ideal system. This generally induces the correlation function to give $\gamma_1(0) < 1$.

Since a good agreement between the position of the minima of $\gamma_1(x)$ and $\gamma_1^*(x)$ was found, we conclude that the reason for the main part of the discrepancy between L_I and L_C is a real effect rather than a mathematical artifact. The reason for this discrepancy has to be sought in the following consideration:

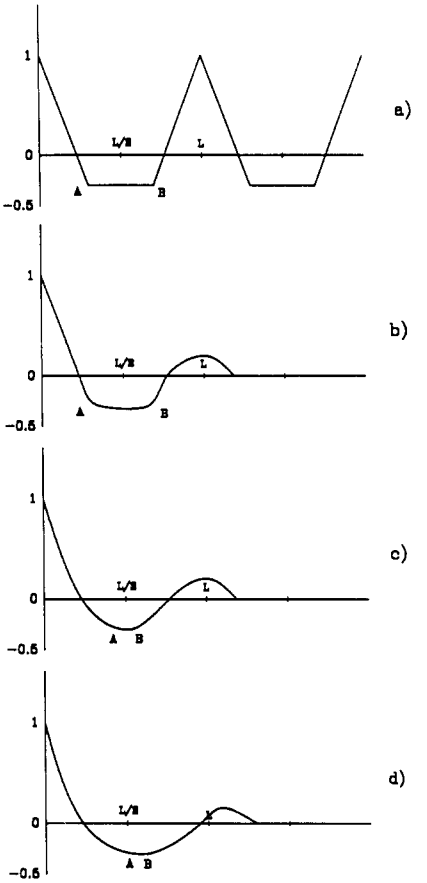

Figure 11. Linear correlation functions of an ideal model (a) and of models with increasing variance in the thickness of the two phases (b–d) (see text).

As was pointed out for example by Strobl,[3] in a system in which l_1 and l_2 have each one single value, the correlation function has a constant value in the range of the position of the minimum (Figure 11a). If the smaller value, l_2, varies from lamellae to lamellae, instead of a sharp corner at point A a smooth change in the slope is observed (Figure 11b). If the larger value, l_1, varies, the sharp corner at the edge B is smoothed. As long as the distributions of the values of l_1 and l_2 are comparatively small, the correlation function as shown in Figure 11b is obtained. In the case of a broad distribution, however, the curve in Figure 11c is found, which shows no region of constant value for $\gamma_1(x)$ and where the value of $\gamma_1(x)$ at the minimum is higher than in Figure 11b. In addition, if the half-widths of the distribution function of l_1 and l_2 are different, the position of the minimum is shifted. The shift occurs to the right side, yielding larger apparent values of L if the distribution function of l_2 is broader than the distribution function of l_1. This is shown in Appendix A, where it is also demonstrated that the value for the long period derived from the first minimum of the correlation function is always larger than the real value.

Now by using the interface distribution function it can be shown[21] that one obtains broad distributions for l_1 and

Table III
Values Obtained for the Invariant by Different Evaluation Procedures[a]

	T_c = 120 °C			T_c = 190 °C			T_c = 240 °C		
t_c, h	1	9	24	1	9	24	1	9	24
Q_1, e²/nm⁶	1488	1532	1466	1580	1619	1526	1525	1464	1521
Q_2, e²/nm⁶	359	380	375	409	459	405	469	468	504
Q_3, e²/nm⁶	440	470	461	481	513	471	520	519	563
Q_4, e²/nm⁶	370	400	400	450	470	450	490	500	555
Q, e²/nm⁶	400	434	410	481	508	473	517	523	563

[a] Q_1: without doing any correction. Q_2: after subtracting the electron density fluctuation. Q_3: after, in addition, extrapolation of the scattering curve to $s = \infty$, assuming sharp phase boundaries. Q_4: after extrapolation of the scattering curve to $s = \infty$ using the method of ref 19. Q: after taking into account all corrections, including finite phase boundaries.

Table IV
Long Period, L, Values Derived from the Correlation Function, L_C^M and L_C^m, from the Interface Distribution Function, L_{IS}, and from the Correlation Function Obtained after Double Integration of the Interface Distribution Function, L_C^{*m} and L_C^{*M}, for the Samples Crystallized for 24 h at the Different Crystallization Temperatures

	L from $\gamma_1(x)$		L from $\gamma_1^*(x)$		L from $g_1(x)$
sample	L_C^m	L_C^M	L_C^{*m}	L_C^{*M}	L_{IS}
240 °C	11.2	11.8	11.2	11.4	8.2
190 °C	9.0	9.4	8.5	9.0	7.3
120 °C	7.2	7.4	6.8	7.0	4.9

l_2 and that the distribution of l_2 is broader than the one of l_1. These are exactly the conditions which lead to the shift of the minimum in the correlation function to larger values.

In the case of our evaluation of the interface distribution function, a broad distribution of l_1 and l_2 lengths does not affect the value of L because we are separating the different distributons as shown in Figure 2. If the different contributions are not separated, incorrect values are also obtained. It can be proved that the value L_I derived from the interface distribution function without separation is always larger than the actual value (see Appendix B).

In summary, the above considerations show that the values of L_{IS}, l_1, and l_2 calculated from the interface distribution function are the most accurate ones. Those derived from the correlation function are shifted to larger values because the distribution of l_1 is smaller than the one of l_2. The values derived from the interface distribution function obviously are not as sensitive to changes caused by a broad distribution function of l_1 and l_2 as the values obtained from the correlation function. This is clearly seen by the fact that even without any separation of the different contributions to $g_1(x)$, the values obtained from $g_1(x)$ are smaller than those obtained from $\gamma_1(x)$ (see Figure 7). The model calculations presented in Appendix B are another proof of this statement. A further advantage in the evaluation of the interface distribution function is the possibility to separate the peaks corresponding to l_1 and l_2 and, thus, to correct for the superposition effects and improve the accuracy in the determination of the average values of l_1 and l_2.

Accuracy in the Measurement of the Invariant Q. As shown in the following section, the interpretation of the results strongly depends on the absolute value of Q. Therefore, we have carefully examined possible errors in the measurement of this quantity.

First, there arises the question of how reliable the moving-slit method is for the determination of the intensity of the primary beam. To verify this point we have reexamined the geometry of the system, including a very careful measurement of the width of the moving slit. Therefore, we can exclude any relevant error in the geometrical constants. In addition, to double check the

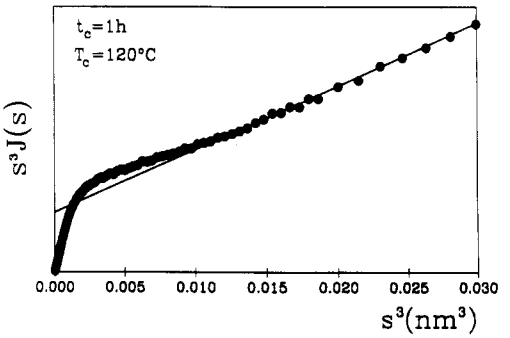

Figure 12. Method of evaluation of the scattering intensity according to Ruland[4] to calculate the electron density fluctuation and Porod's asymptote for the sample crystallized at T_c = 120 °C and t_c = 1 h.

calibration of the camera we used a standard Lupolen sample, which was kindly supplied by Dr. Zipper from the Institut für Feinstrukturforschung in Graz. We found that the moving-slit method yields a Q value which is 1.5% larger than the value obtained by using the external standard Lupolen sample. This inaccuracy is small if compared to the deviations shown in Figure 13, which are of the order of 50%. Therefore, we believe that the calibration of the method is satisfactory.

Second, we have to estimate the errors in the determination of Q caused by the possible inaccurate corrections of the measured scattering curve with respect to local density fluctuations and the finite thickness of the phase boundary and also caused by possible errors in the extrapolation to large scattering angles. To do this we calculate the values of Q from the scattering curves which were only corrected with respect to some of the above-mentioned contributions. Thereafter, the differently obtained values were compared. Let us first calculate Q by integration of the scattering intensity as it was measured in the region s = 0 to s = 0.35 nm⁻¹ without making any correction. The obtained values are denoted by Q_1 and are presented in the first column of Table III.

Let us next take into account the local density fluctuations while the phase boundary is still assumed to be infinitely small and, therefore, of no influence. In this case, according to Ruland,[4] for large values of s the smeared scattering intensity is given by

$$\frac{J(s)}{V} = J_{Fl} + \frac{A_P}{s^3} \tag{16}$$

When $s^3J(s)/V$ is plotted against s^3, a straight line is obtained. One can obtain the A_P value from the intercept and the value of J_{Fl} from the slope. Figure 12 shows, as an example, the corresponding curve for samples crystallized for 1 h at 240 °C. To determine Q, the value of J_{Fl} was subtracted from the measured curve and the remaining intensity was integrated up to s = 0.35 nm⁻¹.

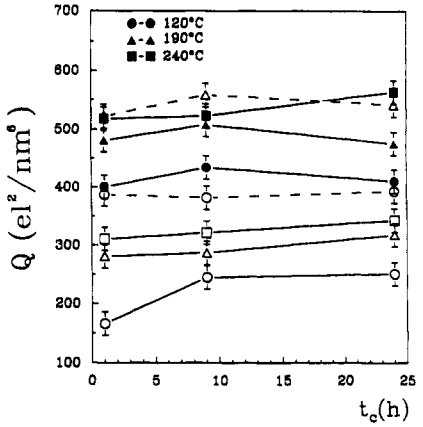

Figure 13. Values of the invariant, Q, for PET samples crystallized at different temperatures as a function of crystallization time. Solid symbols joined by solid lines: Q values obtained by integration of the scattering curves using eq 2. Open symbols joined by solid lines: Q values calculated from eqs 17 and 18 with $x_{CL} \approx 0.7$. Open symbols joined by dashed lines: Q values obtained from eqs 17 and 18 with $x_{CL} \approx 0.3$.

The values of Q thus obtained are denoted by Q_2 and presented in column 2 of Table III.

In a third step we have extrapolated the scattering curve to $s = \infty$ by applying Porod's law. The corresponding Q values (to be called Q_3) are also represented in the table. This extrapolation increases the Q_2 value by 20%.

In another way, we calculated Q by subtracting J_{FI} using the method of Koberstein, Morra, and Stein[19] and after extrapolation to $s = \infty$, however, without the finite phase boundary correction. These values are denoted by Q_4 in Table III.

Finally, the last column in Table III presents the Q values presented in Table II. In this calculation all corrections, including a phase boundary of finite thickness, are taken into account.

By comparing the values of Q obtained in different ways one can see that the differences between Q_2, Q_3, Q_4, and Q are about ±10% while the calculated values of Q represented in Figure 13 by the solid lines are lying 40% below the measured values. Therefore, we believe that the discrepancy between the measured and the calculated values in this figure is not caused by an inaccurate correction of the measured scattering curves with respect to the finite thickness of the phase boundaries or by an incorrect extrapolation of the curve. The contribution of the local electron density fluctuation is, in contrast, comparatively large as can be seen by comparison of Q_1 with the other Q values in Table III. Therefore, in the subtraction of this contribution, in principle, a considerable error may be involved. The amount of possible error in subtracting this contribution can be estimated by comparing Q_4 with Q_3, where J_{FI} is subtracted by using different methods while all other corrections are performed in the same way. One can see that Q_4 is about 20% smaller than Q_3. This difference is still small compared to the difference discussed in connection with Figure 13, where differences of 40% occur. In addition, we wish to point out that by applying the method of Koberstein, Morra, and Stein[19] in calculating Q_4 and Q an upper limit of J_{FI} is obtained, resulting in the smallest possible value of Q. Thus, we believe that any possible error in Q is negligible with respect to the effect discussed in the next sections.

From the above considerations we conclude that there is no systematic error in the measured values of Q.

It is worthy to point out that Fisher and Fakirov[16] have previously found Q values for PET which are about 40% smaller than those reported here. In their evaluation they have neglected the scattering at large angles by subtracting a constant background from the scattering curves. They also subtracted a certain amount of scattering at small angles which they considered to be caused by heterogeneities. Smaller Q values than those reported here were previously found by Konrad and Zachmann,[15] who also neglected the contribution of the scattering at large angles. In addition, one must take into consideration that the PET used in the former publications might have a diethylene glycol content different from that of the samples used in the present study. From the foregoing, we conclude that the difference between the Q values determined earlier and our present data is most probably due to the abovementioned difference in the evaluation method and maybe in the sample used.

Comparison of the Measured Invariant with Calculated Values. For the interpretation of the measured values of the invariant Q we will assume that not all material forms lamellar stacks but only a fraction of it, which we call x_L. Let us recall that x_{CL} is the crystalline fraction and $1 - x_{CL}$ is the amorphous fraction within the stacks. Hence, $1 - x_L$ would be the fraction of the material formed by larger amorphous regions outside the lamellar stacks. Let us take into account two possible models:

First Model. In this model we assume that the fraction $1 - x_L$ does not contribute to Q due to the fact that these larger amorphous regions scatter at such small angles that their scattering cannot be resolved. We, then, can write

$$Q = x_L x_{CL}(1 - x_{CL})(\rho_c - \rho_a)^2 \tag{17}$$

where x_L is given by

$$x_L = x_c/x_{CL} \tag{18}$$

and x_c is the volume degree of crystallinity, which can be calculated from the mass degree of crystallinity, as measured for example by WAXS, by multiplying by ρ/ρ_c. The x_{CL} vaues were obtained from the SAXS correlation function (see Table I); however, it cannot be decided which one of the two values, either x_1 or $1 - x_1$, is identified as x_{CL}.

Figure 13 shows measured and calculated values of the invariant Q as a function of the crystallization time t_c for the the three different crystallization temperatures. We wish to recall that x_1 is the largest of the two values and that x_1 is close to 0.7 for all samples. Finally, the results obtained under the assumption that $x_{CL} = 1 - x_1$ are represented by dashed lines and the corresponding open symbols. As one can see, no matter which one of the two values we choose, there arise ambiguities in explaining the measured Q values in this model:

(a) If one assumes that x_{CL} is equal to $1 - x_1$, a relatively good agreement is obtained for the samples crystallized at 120 °C. It follows that $x_L \approx 0.45$. However, for the samples crystallized at 190 and 240 °C, such an assumption is questionable because in these cases $x_L = x_c/x_{CL}$ would be larger than 1, which, by definition, is not possible. For the sample crystallized at 240 °C for 24 h $x_{CL} = 1 - x_1$ would be 0.32 while x_c is 0.51. This discrepancy is beyond any experimental error.

(b) If, on the other hand, one assumes $x_{CL} = x_1$, the measured values are larger than the calculated ones by a factor 1.8 (see Figure 13). Therefore, this assumption can only be further considered if some changes in the model are introduced. One possibility would be to question the values $\rho_c = 1.490\ g/cm^3$ and $\rho_a = 1.338\ g/cm^3$ and calculate new values for these quantities in such a way that all results were consistent. We have done this by assuming $x_{CL} = x_1$

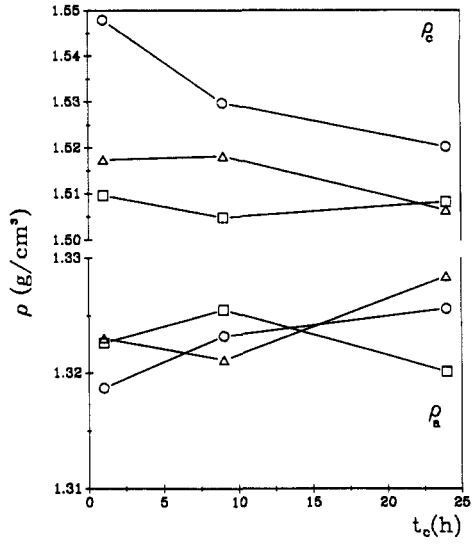

Figure 14. Density of the crystals, ρ_c, and of the amorphous regions, ρ_a, calculated by means of eqs 19–21 for the samples crystallized at different temperatures as a function of crystallization time.

≈ 0.7 and calculating ρ_c and ρ_a by means of the equations

$$Q = x_L x_{CL}(1 - x_{CL})(\rho_c - \rho_a)^2 \tag{19}$$

$$x_L = x_c / x_{CL} \tag{20}$$

$$x_c = \frac{\rho - \rho_a}{\rho_c - \rho_a} \tag{21}$$

where x_c is the volume degree of crystallinity obtained by multiplying the mass degree of crystallinity, measured by WAXS, by ρ/ρ_c.

Figure 14 shows the obtained results. One can see that the values of ρ_c are clearly larger than 1.490 g/cm³ and those for ρ_a much smaller than 1.338 g/cm³. The largest value ever reported for ρ_c is 1.505 g/cm³.[16] Values for ρ_a which are smaller than 1.331 g/cm³ have also been discussed.[15,16] However, such values have never been unambiguously confirmed. In addition, these new values would not agree with the previously observed[9] linear relationship between the density and the degree of crystallinity as determined by WAXS. Therefore, the interpretation of the results by assuming the calculated values of ρ_a and ρ_c remains questionable.

In summary, by applying the model in which only a fraction of material scatters, one can just explain the results on the samples crystallized at lower temperatures. Complete consistency of all data is only obtained if unconventional values of ρ_c and ρ_a were used. Because of the difficulties discussed above, we discard the first model and consider the following a second model.

Second Model. In contrast to the first model, we now assume that both the thickness of the lamellar stacks d_L and the distances between the lamellar stacks d_{IL} (see Figure 15) are so small, let us say $d_L + d_{IL} < 100$ nm, that the scattering arising from the density difference between the regions x_L and $1 - x_L$ is resolved in our measurements and, therefore, contributes to the scattering power Q. This would imply that each coherently scattering lamellar stack consists of not more than 3–6 lamellae. The distances d_L and d_{IL} are randomly distributed so that the scattering arising from the density difference in the regions x_L and $1 - x_L$ is continuously decreasing with increasing scattering angle rather than showing a peak which would correspond

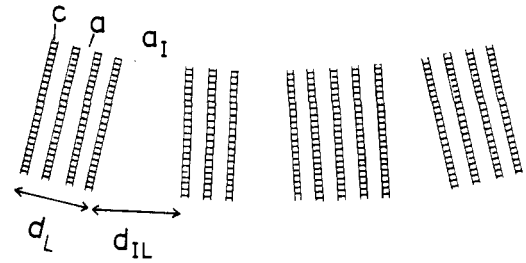

Figure 15. Schematic representation of 4 lamellar stacks consisting of crystals (c), amorphous regions (a), and amorphous regions between the lamellar stacks (a_I).

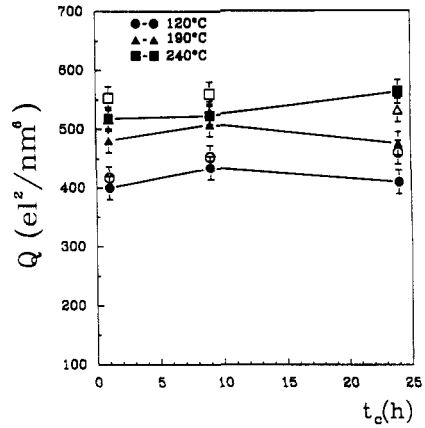

Figure 16. Values of the invariant, Q, for the samples of Figure 13. Solid data joined by solid lines: same as in Figure 13. Open symbols: Q values obtained from eq 22.

to any dominant value of $d_L + d_{IL}$. In this case this additional continuous scattering will not affect the position of the maximum of the correlation function; however, it will increase the value of Q. Actually, because the total material does contribute to Q, the overall degree of crystallinity x_c will determine the value of this quantity, and one obtains

$$Q = x_c(1 - x_c)(\rho_c - \rho_a)^2 \tag{22}$$

The values of Q calculated in this way are presented in Figure 16 together with the experimental values. According to this second model, a fairly good agreement between calculated and experimental results is obtained, though some of the calculated values are lying a little higher than the measured ones. This difference may indicate that a small fraction of the amorphous material lying outside of the lamellar stacks does not contribute to the scattering intensity. Indeed, the good agreement between the calculated and the measured values of Q shows that eq 22 rather than eq 19 gives the correct results.

Electron microscopic investigations[12] support our conclusion that there exist larger amorphous regions of irregular size between the lamellar stacks. The amount of these amorphous regions disturbing the regular arrangement of the lamellae decreases with increasing temperature of crystallization T_c. This corresponds to the increase of x_L with T_c in our model.

Conclusions

In the case of broad distributions of the values of the crystal thickness (l_c), amorphous thickness (l_a), and the long period (L), these parameters can be determined with higher accuracy from the interface distribution function than from the correlation function. The reason for this is that the interface distribution function is less affected by the superposition of the maxima or minima of a broad distribution than the relevant shape of the correlation

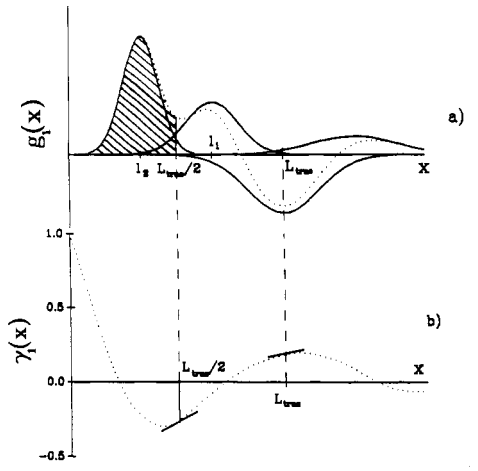

Figure 17. Schematic representation of the interface distribution function and of the correlation function to illustrate the influence of the thickness distribution of the different regions on the first derivative of the correlation function (see text).

function. The L values obtained by simply applying Bragg's law are considerably larger than the true values. The distribution of the values of crystal thickness and long period is very broad.

It is found that the crystalline fraction within the lamellar stacks x_{CL} is considerably larger than the overall degree of crystallinity x_c, in agreement with earlier findings.[15] The value of x_{CL} is almost independent of the time and temperature of crystallization and turns out to be approximately equal to 0.7.

The results obtained favor the view that the lamellar stacks consist of only 3–6 coherently scattering crystal lamellae and that there exist amorphous regions outside of the lamellar stacks which are larger than those within the lamellar stacks but still small enough to contribute to the detected diffuse small-angle X-ray scattering. The fraction of these regions, $1 - x_c/x_1$, decreases with increasing temperature of crystallization.

Acknowledgment. We express our thanks to the Internationales Büro, Kernforschunganlage, Kalsruhe, and to CSIC, Madrid, for the generous support of this cooperation project. Grateful acknowledgment is also due to CICYT, Spain, for the support of this investigation (Grant MAT88-0159). H.G.Z. thanks the Secretaría de Estado de Universidades e Investigación, Spain, for the award of the Humboldt-Mutis Prize by which this work was also supported.

Appendix A: Theoretical Considerations

In what follows we want to demonstrate that (1) the long period L_C^M derived from the first maximum of the correlation function is always larger than the true average value, L_{true}, and (2) the long period L_C^m derived from the first minimum of the correlation function is smaller than L_{true} if $\sigma_1 > \sigma_2$, where σ_i is the variance of the distance l_i and l_1 is the larger distance in the two-phase system. If $\sigma_1 < \sigma_2$ then $L_C^m > L_{true}$.

To prove the above statement, we have to calculate the first derivative of the correlation function $\gamma_1'(x)$ at $x = L_{true}/2$ and at $x = L_{true}$.

Concerning the first statement, one can see from Figure 17 that

$$\text{if } L_C^M > L_{true} \Leftrightarrow \gamma_1'(L_{true}) > 0 \tag{23}$$

Concerning the second state, one recognizes in the same way that

$$\text{if } L_C^m > L_{true} \Leftrightarrow \gamma_1'(L_{true}/2) < 0 \tag{24}$$

and

$$\text{if } L_C^m < L_{true} \Leftrightarrow \gamma_1'(L_{true}/2) > 0 \tag{25}$$

To demonstrate the above statements, we use the equation

$$\gamma_1''(x) = g_1(x) \tag{26}$$

and obtain

$$\gamma_1'(x) = \gamma_1'(0) + \int_0^x g_1(u)\,du \tag{27}$$

where $\gamma_1'(0) < 0$ and $g_1(u)$ is the sum of the distributions for l_2, l_1, L, and so on[4,5] (Figure 17); i.e.

$$g_1(u) = -\gamma_1'(0)(h_2(u) + h_1(u) - 2h_L(u) + \ldots + \text{2nd order}) \tag{28}$$

where $h_i(u)$ is the normalized Gaussian function with an average value equal to l_i and variance equal to σ_i.

From eq 27 one can obtain

$$\gamma_1'(L_{true}/2) = \gamma_1'(0) + \int_0^{L_{true}/2} g_1(u)\,du \tag{29}$$

Depending on the values of the individual variances we have three alternatives:

1. If σ_1, σ_2, and σ_L are sufficiently small, then there is no superposition of the individual distributions, and from the shaded area of Figure 17 and from eq 29 one can deduce that $\gamma_1'(L_{true}/2) = 0$. Thus the correct value for the long period is obtained.

2. If $\sigma_2 > \sigma_1$, then a part of the area which corresponds to the distribution of l_2 is not taken into account in the integral of eq 29 and the tail of the l_1 distribution is not so large as to compensate the loss of area from the l_2 distribution. In this case, more integrated area is lost than is gained. Therefore

$$\gamma_1'(L_{true}/2) = \gamma_1'(0) - k\gamma_1'(0) < 0 \tag{30}$$

with $0 < k < 1$. This means that using eq 24 one obtains a value for the long period, $L_C^m > L_{true}$.

3. If $\sigma_2 < \sigma_1$, more integrated area is gained than is lost. Therefore

$$\gamma_1'(0) = -\gamma_1'(0)(k' - 1) > 0 \tag{31}$$

with $0 < k' < 1$. This means that using eq 25 one obtains $L_C^m < L_{true}$.

One can follow the same procedure to obtain the value $\gamma_1'(L_{true})$. This is given by

$$\gamma_1'(L_{true}) = \gamma_1'(0) + \int_0^{L_{true}} g_1(u)\,du \tag{32}$$

This integral corresponds to the following contributions: (a) the whole area of the l_2 distribution (i.e., $-\gamma_1'(0)$), (b) the whole area of the l_1 distribution (i.e., $-\gamma_1'(0)$), (c) half the area of the L distribution, which represents $+\gamma_1'(0)$ because it has double weight, and (d) the tail of the $L + l_2$ distribution, which represents $-k\gamma_1'(0)$ and $0 < k < 1$. Then one obtains for $\gamma_1'(L_{true})$

$$\gamma_1'(L_{true}) = \gamma_1'(0) - \gamma_1'(0) - \gamma_1'(0) + \gamma_1'(0) - k\gamma_1'(0) = -k\gamma_1'(0) > 0 \tag{33}$$

By using eq 23, it follows that $L_C^M > L_{true}$.

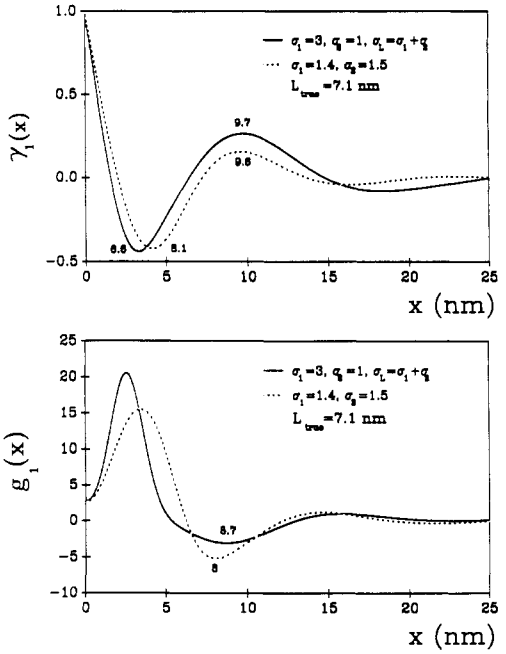

Figure 18. Model calculations of the correlation function and the interface distribution function using different values for σ_i.

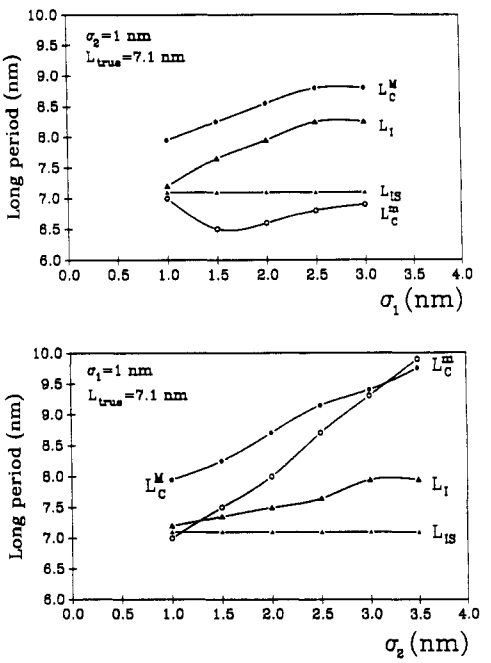

Figure 19. Influence of the variances σ_1 and σ_2 upon the values of the long periods L_I, L_{IS}, L_C^M, and L_C^m obtained by different evaluation methods.

Appendix B: Model Calculations

We have calculated the correlation function and the interface distribution function for an ideal two-phase system with an average long period L_{true} = 7.1 nm and average thickness of phase 1 l_1 = 4.5 nm and of phase 2 l_2 = 2.7 nm. The variances σ_1 and σ_2 for the respective distributions of l_1 and l_2 were changed between 1 and 3 nm. It was further assumed that $\sigma_L = \sigma_1 + \sigma_2$.

As an example Figure 18 shows the correlation function and the interface distribution function for two different values of the variances. One can see that both the first minimum and the first maximum in the correlation function are very much affected by changing the values of the variances. The same shift occurs for the first minimum in the interface distribution function. The results obtained for L_C^m, L_C^M, L_I, and L_{IS} for the different values of the variance are presented in Figure 19. Figure 19 (top) shows the values obtained by letting constant σ_2 and varying σ_1, while Figure 19 (bottom) gives the values assuming σ_1 = constant and varying σ_2. The main conclusions in this case are as follows:

(i) The value of the long period from the interface distribution function after doing the separation of the different contributions (L_{IS}) is always equal to the real value. $L_{IS} = L_{true}$.

(ii) The value for the long period from the first minimum of the interface distribution function (L_I) is always larger than the real value and is affected by the different values of the variances. $L_I > L_{true}$.

(iii) The value for the long period from the first maximum of the correlation function (L_C^M) is always larger than the real value and it is more affected by the different values of the variances than L_I. $L_C^M > L_I > L_{true}$.

(iv) The value for the long period obtained from the first minimum of the correlation function (L_C^m) is smaller than the real value if the variance of the larger thickness is larger than the variance for the smaller thickness and vice versa. $L_C^m < L_{true}$ if $\sigma_1 > \sigma_2$ and $L_C^m > L_{true}$ if $\sigma_1 < \sigma_2$.

(v) If the variances for the two thickness distributions ($\sigma_1 = \sigma_2$) are the same, then the long period obtained from the first minimum of the correlation function and the one obtained from the first minimum of the interface distribution function are nearly equal to the true value. $L_C^m \approx L_I \approx L_{true}$ when $\sigma_1 = \sigma_2$.

References and Notes

(1) Kortleve, G.; Vonk, C. G. *Kolloid-Z.* **1968**, *225*, 124.
(2) Vonk, C. G.; Kortleve, G. *Kolloid-Z.* **1967**, *220*, 19.
(3) Strobl, G. R.; Schneider, M. *J. Polym. Sci.* **1980**, *18*, 1343.
(4) Ruland, W. *Colloid Polym. Sci.* **1977**, *255*, 417.
(5) Stribeck, N.; Ruland, W. *J. Appl. Crystallogr.* **1978**, *11*, 535.
(6) Morgan, L. B.; Keller, A. Lester *Philos. Trans. R. Soc. London* **1954**, *A247*, 1, 13, 23.
(7) Zachmann, H. G.; Stuart, H. A. *Makromol. Chem.* **1960**, *41*, 131.
(8) Zachmann, H. G.; Stuart, H. A. *Makromol. Chem.* **1960**, *41*, 148.
(9) Gehrke, R.; Zachmann, H. G. *Makromol. Chem.* **1981**, *182*, 627.
(10) Zachmann, H. G.; Smith, G. F. *Makromol. Chem.* **1961**, *52*, 23.
(11) Elsner, G.; Koch, M. H. J.; Bordas, J.; Zachmann, H. G. *Makromol. Chem.* **1981**, *182*, 126.
(12) Groeninckx, G.; Reynaers, H.; Berghmans, H.; Smets, G. *J. Polym. Sci.* **1980**, *18*, 1311.
(13) Zachmann, H. G.; Gehrke, R. In *Morphology of Polymers*; Sedlácek, Ed.; Walter de Gruyter: Berlin, New York, 1986; p 119.
(14) Gehrke, R.; Riekel, C.; Zachmann, H. G. *Polymer* **1989**, *30*, 1582.
(15) Konrad, G.; Zachmann, H. G. *Kolloid-Z.* **1971**, *247*, 851.
(16) Fisher, E. W.; Fakirov, S. *J. Mater. Sci.* **1976**, *11*, 1041.
(17) Berkowitz, S. *J. Appl. Polym. Sci.* **1984**, *29*, 4353.
(18) Stabinger, H.; Kratky, O. *Makromol. Chem.* **1978**, *179*, 1655.
(19) Koberstein, J. T.; Morra, B.; Stein, R. S. *J. Appl. Crystallogr.* **1980**, *13*, 34.
(20) Baltá Calleja, F. J.; Vonk, C. G. *X-ray Scattering of Synthetic Polymers*; Elsevier: Amsterdam, 1989; p 248.
(21) Stribeck, N.; Santa Cruz, C., to be published.

Registry No. PET, 25038-59-9.